

# Onsager-Kraichnan Condensation in Decaying Two-Dimensional Quantum Turbulence

T. P. Billam,<sup>1,\*</sup> M. T. Reeves,<sup>1</sup> B. P. Anderson,<sup>2</sup> and A. S. Bradley<sup>1,†</sup>

<sup>1</sup>*Jack Dodd Centre for Quantum Technology, Department of Physics, University of Otago, Dunedin 9016, New Zealand*

<sup>2</sup>*College of Optical Sciences, University of Arizona, Tucson, Arizona 85721, USA*

(Received 24 July 2013; revised manuscript received 10 March 2014; published 11 April 2014)

Despite the prominence of Onsager's point-vortex model as a statistical description of 2D classical turbulence, a first-principles development of the model for a realistic superfluid has remained an open problem. Here we develop a mapping of a system of quantum vortices described by the homogeneous 2D Gross-Pitaevskii equation (GPE) to the point-vortex model, enabling Monte Carlo sampling of the vortex microcanonical ensemble. We use this approach to survey the full range of vortex states in a 2D superfluid, from the vortex-dipole gas at positive temperature to negative-temperature states exhibiting both macroscopic vortex clustering and kinetic energy condensation, which we term an *Onsager-Kraichnan condensate* (OKC). Damped GPE simulations reveal that such OKC states can emerge dynamically, via aggregation of small-scale clusters into giant OKC clusters, as the end states of decaying 2D quantum turbulence in a compressible, finite-temperature superfluid. These statistical equilibrium states should be accessible in atomic Bose-Einstein condensate experiments.

DOI: 10.1103/PhysRevLett.112.145301

PACS numbers: 67.85.De, 03.75.Lm, 47.27.-i

The importance of the point-vortex model as a statistical description of two-dimensional (2D) classical hydrodynamic turbulence was identified by Onsager [1], who predicted that the bounded phase space of a system of vortices implies the existence of negative-temperature states exhibiting clustering of like-circulation vortices [2]. This model provides great insight into 2D classical turbulence (CT) [3], and much subsequent work has focused on the point-vortex model as an approximate statistical description of decaying 2DCT [4–8]. While classical fluids cannot directly realize the point-vortex model, atomic Bose-Einstein condensates (BECs)—which present an emerging theoretical [9–23] and experimental [24–26] paradigm system for the study of quantum vortices and 2D quantum turbulence (2DQT)—offer the possibility of physically realizing Onsager's negative-temperature equilibrium states. A concrete realization of the point-vortex model in an atomic superfluid will broaden our understanding of the universality of 2D turbulence by enabling new studies of spectral condensation of energy at large scales [27–30], statistical mechanics of negative-temperature states [31–33], the dynamics of macroscopic vortex clustering [34], and the inverse energy cascade [35–38], previously confined to 2DCT.

In this Letter we develop an analytic statistical description of the microstates of 2D quantum vortices within the homogeneous Gross-Pitaevskii theory, and show that macroscopically clustered vortex states emerge from small-scale initial clustering as end products of decaying 2DQT. As in CT, the homogeneous system offers the clearest insight into the underlying physics, and is increasingly relevant experimentally [39]. Consequently, our results describe physics relevant to a wide range of possible vortex

experiments in atomic BECs. By systematically sampling the microcanonical ensemble for the vortex degrees of freedom, we give a detailed, unifying view of the properties of vortex matter in a homogeneous 2D superfluid. We characterize the emergence of macroscopic clusters of quantum vortices at negative temperatures, linked with spectral condensation of energy at the system scale. In the context of 2DQT we call this the *Onsager-Kraichnan condensate* (OKC), as it represents a physically realizable state that unifies Onsager's negative-temperature point-vortex clusters with the spectral condensation of kinetic energy predicted in 2DCT by Kraichnan [27].

Atomic BECs support quantum vortices subject to thermal and acoustic dissipative processes that may be detrimental to the observation of an OKC. We assess the accessibility of the excited states comprising an OKC via dynamical simulations according to the damped Gross-Pitaevskii equation (dGPE). We find that our statistical approach describes the end states of decaying 2DQT that emerge dynamically from low-entropy initial states. Even for relatively small positive point-vortex energies, the OKC emerges as a result of statistically driven transfer of energy to large length scales.

To map the Gross-Pitaevskii theory to the point-vortex model, we introduce an ansatz wave function for  $N$  vortices in a homogeneous periodic square BEC of side  $L$ , with positions  $\mathbf{r}_j$  and circulations  $h\kappa_j/m$  defined by charges  $\kappa_j = \pm 1$  ( $\sum_{j=1}^N \kappa_j = 0$ ),

$$\psi(\mathbf{r}, \{\mathbf{r}_j\}, \{\kappa_j\}) = e^{i\theta(\mathbf{r}, \{\mathbf{r}_j\}, \{\kappa_j\})} \prod_{p=1}^N \chi(|\mathbf{r} - \mathbf{r}_p|), \quad (1)$$

where  $\chi(r)$  is the radial profile of an isolated quantum vortex core, obtained numerically [19]. Unlike the velocity

field for point vortices in a doubly-periodic domain [31,32], the associated quantum phase  $\theta$  does not, to our knowledge, appear in the literature. We present an expression for  $\theta$  as a rapidly convergent sum, obtained from a poorly convergent sum over periodic replica vortices, in the Supplemental Material [40]. The phase  $\theta$  yields a periodic superfluid velocity  $\mathbf{v} = (\hbar/m)\nabla\theta$  very close to the point-vortex velocity, but consistently modified by the boundary conditions such that  $\theta(x + \eta_x L, y + \eta_y L) = \theta(x, y) + \zeta 2\pi$ , for all  $\eta_x, \eta_y, \zeta \in \mathbb{Z}$ , remains a well-defined quantum phase. To ensure that  $\chi(r)$  is accurate, we enforce a minimum-separation constraint  $|\mathbf{r}_p - \mathbf{r}_q| \geq 2\pi\xi$ , where  $\xi = \hbar/\sqrt{\mu m}$  is the healing length (for BEC chemical potential  $\mu$  and atomic mass  $m$ ), and  $1 \leq p \neq q \leq N$ .

Up to an additive constant, the total kinetic energy in the point-vortex model is  $N\Omega_0\xi^2\epsilon(\{\mathbf{r}_j\}, \{\kappa_j\})$ . Here, the dimensionless point-vortex energy (per vortex) is given by [32]

$$\epsilon(\{\mathbf{r}_j\}, \{\kappa_j\}) = \frac{1}{N} \sum_{p=1}^{N-1} \sum_{q=p+1}^N \kappa_p \kappa_q f\left(\frac{\mathbf{r}_p - \mathbf{r}_q}{L}\right), \quad (2)$$

where  $f(\mathbf{r}) \equiv f(x, y) = 2\pi[|y|(|y|-1) + 1/6] - \log\{\prod_{s=-\infty}^{\infty} [1 - 2\cos(2\pi x)\exp(-2\pi|y+s|) + \exp(-4\pi|y+s|)]\}$ , and  $\Omega_0 = \pi\hbar^2 n_0/m\xi^2$  is the unit of enstrophy for 2D homogeneous superfluid density  $n_0$  [19]. Accounting for compressible effects with the core ansatz  $\chi_\Lambda(r) = [n_0 r^2/(r^2 + \xi^2 \Lambda^{-2})]^{1/2}$ , the incompressible kinetic energy (IKE) spectrum of Eq. (1) at scales below the system size  $L$  is well approximated by [19,40]

$$E^i(k) = \Omega_0 \xi^3 F_\Lambda(k\xi) \left[ N + 2 \sum_{p=1}^{N-1} \sum_{q=p+1}^N \kappa_p \kappa_q J_0(k|\mathbf{r}_p - \mathbf{r}_q|) \right], \quad (3)$$

where  $F_\Lambda(k\xi) = \Lambda^{-1}g(k\xi\Lambda^{-1})$ ,  $g(z) = (z/4)[I_1(z/2) \times K_0(z/2) - I_0(z/2)K_1(z/2)]$ ,  $\Lambda = \xi^2 n_0^{-1/2} d\chi(0)/dr \approx 0.825$  and  $J_\alpha(I_\alpha, K_\alpha)$  are (modified) Bessel functions. Equation (3) leads to a universal ultraviolet (UV,  $k \gg \xi^{-1}$ )  $k^{-3}$  power law,  $E^i(k) = C(k\xi)^{-3}$ , where  $C = \Lambda^2 N \Omega_0 \xi^3$  [17,19]. In the infrared (IR,  $k \lesssim \xi^{-1}$ ) the average spectrum of  $N$ -vortex configurations with randomly distributed vortices is equal to the sum of  $N$  independent single-vortex spectra, giving the  $k^{-1}$  power law  $E^i(k) = C(k\xi)^{-1}/\Lambda^2$  [17,19,21].

The wave function  $\psi$  [Eq. (1)] is set entirely by the vortex configuration, allowing us to adopt a statistical treatment where, for each configuration  $(\{\mathbf{r}_j\}, \{\kappa_j\})$ ,  $\psi$  defines a microstate of the 2D BEC [54]. Aside from the minimum-separation constraint, the phase  $\theta$  in Eq. (1) establishes a one-to-one correspondence between the  $N$ -vortex states of a 2D BEC and the microstates of the classical point-vortex model. The set of all microstates  $\psi$  at fixed point-vortex energy  $\epsilon$  [Eq. (2)] defines a microcanonical ensemble; the measure of this set is the

structure function  $W(\epsilon)$  (which defines the system entropy  $S(\epsilon) = k_B \ln[W(\epsilon)]$ ). The normalized structure function,  $w(\epsilon) \equiv W(\epsilon)/[\int d\epsilon W(\epsilon)]^{-1}$ , is obtained numerically as a histogram of  $\epsilon$  for random vortex configurations. We sample the microcanonical ensemble at energy  $\epsilon$  numerically, using a random walk to generate many  $N$ -vortex configurations having energies within a given tolerance [58]. Related microcanonical sampling techniques have previously been applied to the classical point-vortex model [31–34]. Averages of observables over this ensemble are dominated by the most likely (highest-entropy) configurations. For large  $N$  (ensuring ergodicity [31,32]) ensemble averages define a statistical equilibrium corresponding to time-averaged properties of the end states of decaying quantum vortex turbulence at energy  $\epsilon$ .

To demonstrate that quantum vortices in a 2D BEC can provide a physical realization of negative-temperature states exhibiting macroscopic vortex clustering, we sample the GPE microstates of the 2D BEC, compute the IKE spectrum, and decompose the vortex configurations into dipoles and clusters using the recursive cluster algorithm (RCA) developed in Ref. [23]. For each cluster the RCA yields the cluster charge  $\kappa_c$  and average radius  $r_c$  (average distance of constituent vortices from the cluster center of mass). We define the clustered fraction  $f_c = \sum_s |\kappa_{c,s}|/N$ , where  $\kappa_{c,s}$  is the charge of the  $s$ th cluster. We also define  $N_{\kappa_c}$  as the total number of vortices participating in all clusters of charge  $\pm|\kappa_c|$ . Finally, we introduce the correlation functions  $c_B = \sum_{p=1}^N \sum_{q=1}^B \kappa_p \kappa_p^{(q)} / BN$ , where  $\kappa_p^{(q)}$  is the charge of the  $q$ th nearest-neighbor to vortex  $p$ . These are directly related to the functions  $C_B$  introduced in Ref. [20]; a value of  $c_B > 0$  ( $< 0$ ) indicates (anti-)correlation between vortex charges, up to the nearest neighbors of  $B$ th order.

Figure 1(a) shows  $w(\epsilon)$  for  $N = 384$  vortices in a doubly periodic box of side  $L = 512\xi$ . The boundary between positive- and negative-temperature states,  $\epsilon_\infty$ , lies at the maximum of  $W(\epsilon)$ , where the temperature  $T = W(\partial W/\partial \epsilon)^{-1}/k_B \rightarrow \infty$ . We find  $\epsilon_\infty \approx -0.255$  and the mean energy  $\langle \epsilon \rangle = 0$  known from the point-vortex model [32] despite the minimum-separation constraint. Figure 1 also shows the averages of the clustering measures [Figs. 1(a),1(b)], the IKE spectrum [Fig. 1(c)], and the distribution of  $N_{\kappa_c}$  [Fig. 1(d)] as a function of  $\epsilon$ . At  $\epsilon = 0$ ,  $c_B$  ( $f_c$ ) is equal to 0 (1/2), indicating an uncorrelated vortex distribution. The distribution of  $N_{\kappa_c}$  is strongly skewed towards small clusters, with  $|\kappa_c|^{\max} < 20$  and  $r_c^{\max} < 50\xi \ll L$ , and the IKE spectrum follows the  $k^{-1}$  law in the IR region. At energies  $\epsilon < 0$  (where  $T > 0$  for  $\epsilon \leq \epsilon_\infty$ ),  $c_B$  ( $f_c$ ) drops below 0 (1/2), indicating proliferation of vortex dipoles and reduced number, charge, and radius of vortex clusters. As  $\epsilon \rightarrow -3$  one obtains a vortex-dipole gas with approximately the minimal spacing  $2\pi\xi$  [see Fig. 2(a)]. The IKE spectrum lies below the  $k^{-1}$  law at large scales. At energies  $\epsilon > 0$  (where  $T < 0$ ) Fig. 1 shows macroscopic vortex clustering and spectral condensation

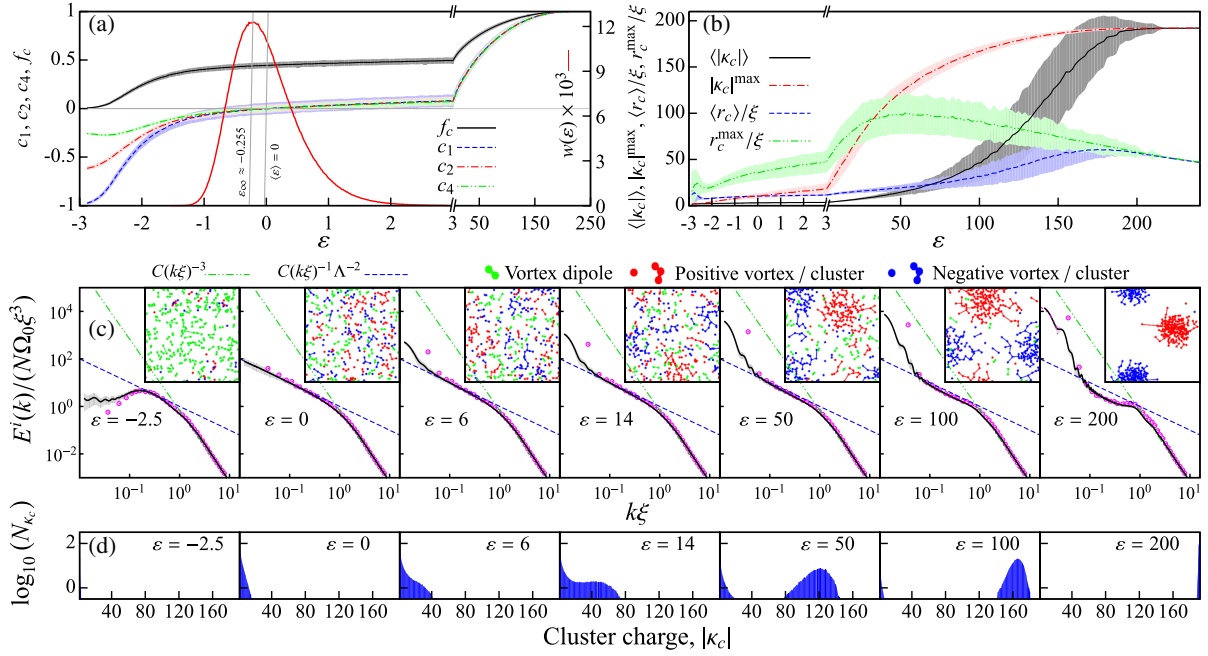


FIG. 1 (color online). Properties of neutral  $N$ -vortex states in statistical equilibrium, corresponding to the end states of decaying 2DQT. (a) Clustering measures  $f_c$  and  $c_B$  and structure function  $w(\epsilon)$ ; vertical gray lines indicate the expected energy ( $\langle \epsilon \rangle$ ) and the boundary between positive- and negative-temperature states ( $\epsilon_{\infty}$ ). (b) Average and maximum cluster charges ( $|\kappa_c|$ ) and radii ( $r_c$ ) obtained using the RCA (see text). (c) IKE spectrum in the point-vortex-like approximation [Eq. (3)] (solid black line, gray shaded area), and obtained from the GPE wave functions [13,19] (magenta circles). Straight lines show analytical  $k^{-3}$  and  $k^{-1}$  power laws (see text). Inset: typical vortex configurations (field of view  $L \times L$ ): dots indicate vortices, which have been sorted into dipoles, free vortices and clusters by the RCA (see legend). Lines show the minimal spanning tree of clusters and identify dipoles. (d) Distribution of  $N_{\kappa_c}$ . Shaded areas behind curves in (a),(b),(c) indicate the width of the equilibrium distribution ( $\pm 1$  standard deviations). Ensemble sizes are given in [58].

of IKE. While low-order measures of clustering ( $c_B$ ,  $f_c$ ) increase slowly with  $\epsilon$ , the distribution of vortices bifurcates, revealing the appearance of two (opposite-sign) macroscopic clusters. Spectrally, the energy associated with these clusters manifests itself as an OKC lying above the  $k^{-1}$  power law at large scales. The charge and radius of clusters ( $|\kappa_c|^{\max}$  and  $r_c^{\max}$ ) grows more rapidly with  $\epsilon$  than  $\langle |\kappa_c| \rangle$  and  $\langle r_c \rangle$  up to  $\epsilon \sim 50$ , highlighting the utility of the RCA for the characterization of point-vortex states. Above this energy, clusters increase in charge less rapidly, and absorb further energy by shrinking in radius. For  $\epsilon \gtrsim 200$  two clusters contain all the vortices, illustrating the phenomenon of supercondensation [28]; in this regime the  $k^{-1}$  spectrum vanishes.

In contrast to the UV-divergent point-vortex model, the universal  $k^{-3}$  UV asymptotic of the IKE spectrum [Eq. (3)] implies a *physical* transition energy for the emergence of the OKC, given by  $E_0 \equiv E_{\text{tot}}^i(\epsilon = 0)$ , where  $E_{\text{tot}}^i(\epsilon) \equiv \int dk E^i(k)$ . An analytic estimate of  $E_0$  follows from the second term in Eq. (3) averaging to zero at  $\epsilon = 0$  ( $c_B = 0$  for all  $B$ ); correctly accounting for the discrete nature of the spectrum [40] yields  $E_0 \approx 4.735N\Omega_0\xi^2$ , in good agreement with the numerical value  $E_0 \approx 4.821N\Omega_0\xi^2$  obtained from  $\psi$ , which does not rely on the core ansatz used to obtain Eq. (3). We find that the total IKE is very well predicted by  $E_{\text{tot}}^i(\epsilon) = E_0 + \epsilon N\Omega_0\xi^2$ . Thus, the appearance

of the OKC is due to the saturation of excited states: IKE exceeding  $E_0$  accumulates near the system scale, forming the spectral feature lying above the  $k^{-1}$  spectrum. Note that the OKC is a (quasi-)equilibrium phenomenon distinct from the classical scenario of condensation in *forced* turbulence, where the  $k^{-5/3}$  spectrum of the inverse energy cascade (IEC) gives way to  $k^{-3}$  at low  $k$  associated with the dynamical condensate [29,30,59].

To demonstrate that Fig. 1 provides a quantitative description of decaying QT in a 2D BEC, and that statistically-driven transfers of energy to large length scales can occur in a *compressible* quantum fluid, we consider the dynamics of nonequilibrium states in the dGPE [60–62]. For a 2D BEC (subject to tight harmonic confinement in the  $z$  direction with oscillator length  $l_z$ ) this can be written as

$$i\hbar \frac{\partial \psi(\mathbf{r}, t)}{\partial t} = (1 - i\gamma) \left( -\frac{\hbar^2 \nabla_{\perp}^2}{2m} + g_2 |\psi(\mathbf{r}, t)|^2 - \mu \right) \psi(\mathbf{r}, t), \quad (4)$$

where  $g_2 = \sqrt{8\pi} \hbar^2 a_s / m l_z$ ,  $m$  is the atomic mass, and  $a_s$  is the  $s$ -wave scattering length. The dimensionless damping rate  $\gamma$  describes collisions between condensate atoms and noncondensate atoms, an important physical process in real 2D superfluids that leads to effective viscosity [19] and suppression of sound energy at high  $k$ . We use the

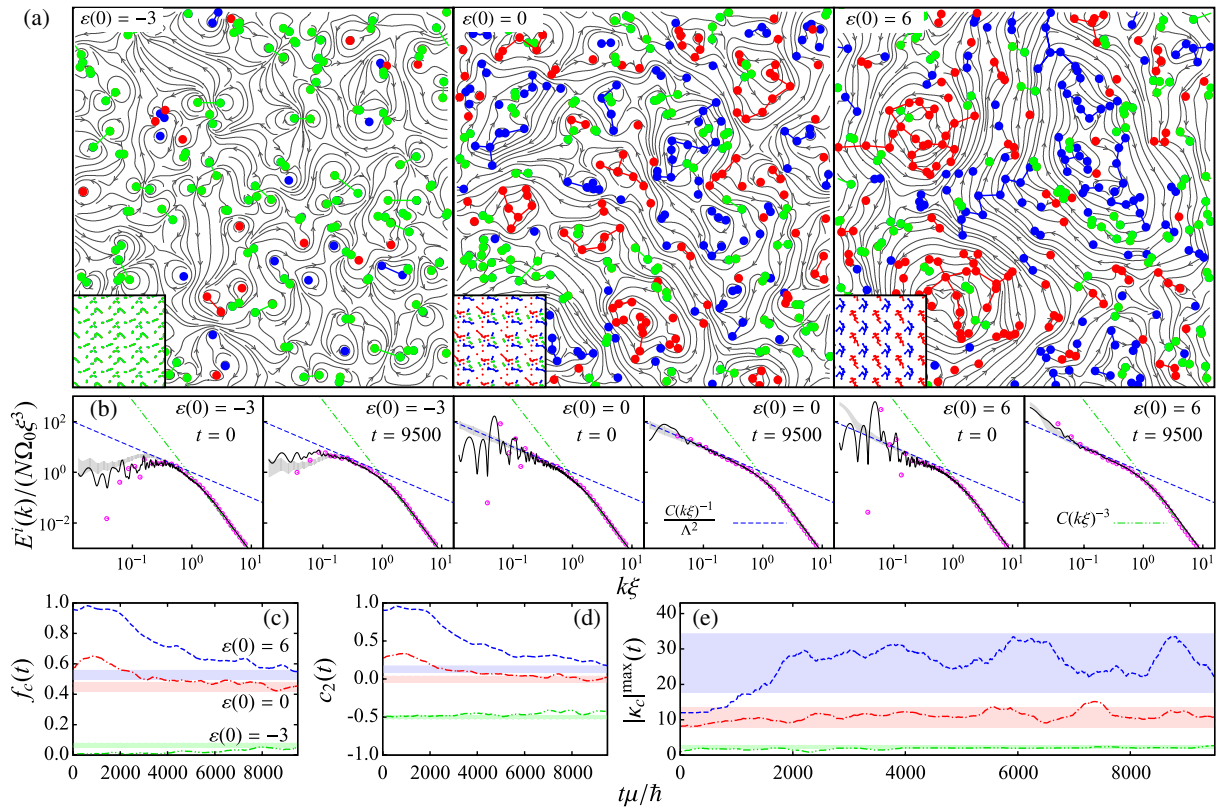


FIG. 2 (color online). Dynamical dGPE evolution of nonequilibrium neutral  $N$ -vortex states towards statistical equilibrium (see also animations in [40]). (a) RCA decomposition after equilibration ( $t = 9500\hbar/\mu$ ), with initial conditions inset. Streamlines show the incompressible velocity field. Field of view is  $L \times L$ . (b) IKE spectrum, compared to the statistical equilibrium distribution from Fig. 1(c) (gray solid line, thickness indicates  $\pm 1$  standard deviations). Other symbols in (a),(b) as in Fig. 1(c). (c) Clustered fraction  $f_c$ . (d) Correlation function  $c_2$ . (e) Absolute charge  $|\kappa_c|$  of the largest vortex cluster. Spectra and measures are shown as a moving average from  $t$  to  $t + 500\hbar/\mu$ , and  $E^i(k)$  is normalized by  $N(t)$ ; decay of  $N(t)$  for  $\varepsilon(0) > -3$  is negligible ( $\lesssim 5\%$ ). Horizontal shading in (c)–(e) shows the statistical equilibrium distributions from Figs. 1(a) and 1(b) (shaded areas indicate  $\pm 1$  standard deviations). Note that we compare the  $\varepsilon(0) = -3$  evolution to the statistical equilibrium at  $\varepsilon = -2.5$ , since dipole annihilation [for  $\varepsilon = -3$ ,  $N(10^4) = 178$ ] leads to  $\varepsilon(10^4) \approx -2.5$ .

experimentally realistic value  $\gamma = 10^{-4}$  [25] in our simulations. We use a random walk to obtain a neutral configuration of  $N' = 24$  vortices in a periodic box of length  $L' = 128\xi$  at energy  $\varepsilon'$ . A  $4^2$  tiling of this configuration, with each vortex subject to Gaussian position noise (variance  $\xi$ ), provides a nonequilibrium, low-entropy state of  $N = 384$  vortices in a box with  $L = 512\xi$  and energy  $\varepsilon$  (found by adjusting  $\varepsilon'$ ). This state is then evolved to time  $10^4\hbar/\mu$  in the dGPE, over which time we find that the compressible energy does not increase [and  $\varepsilon(t)$  does not decay] significantly, supporting our statistical description [63].

Figure 2 shows the time evolution of the vortex configuration for three different initial energies [Fig. 2(a)] with IKE spectra [Fig. 2(b)] and clustering measures [Figs. 2(c)–2(e)] determined by short-time averaging of individual runs of the dGPE. While the approach to complete equilibrium is slow, Fig. 2(e) shows that the charge of the largest cluster equilibrates more rapidly (by  $t \sim 2000\hbar/\mu$ ). For  $\varepsilon(0) = -3$ , the dynamics consists largely of dipole-dipole collisions and vortex-antivortex

annihilation (increasing the energy per vortex  $\varepsilon$ , [32]), and exhibits a time-invariant IKE spectrum; these positive-temperature point-vortex states have no analog in 2DCT [32]. For  $\varepsilon(0) = 0$ , the approach to equilibrium involves significant dipole-cluster interactions that redistribute the cluster charges, decreasing  $f_c$  and  $c_B$  while increasing  $|\kappa_c|^{\max}$ . This redistribution transfers energy to large scales, producing an approximate  $k^{-1}$  power law in the IR [note that the time-averaged spectrum is expected to fluctuate relative to the  $10^4$ -configuration average in Fig. 1(c)]. For  $\varepsilon(0) = 6$  the dynamics is reminiscent of 2DCT. Energy transfer to large scales builds an OKC, with the vortices grouping into two macroscopic clusters [64]. Although a steady  $k^{-5/3}$  spectrum is absent (and would require continuous forcing and damping to establish a steady inertial range [23]) some intermittent  $k^{-5/3}$  behavior is evident [40]. The equilibrium distribution of vortices outside of the OKC closely resembles the uncorrelated ( $\varepsilon = 0$ ) state [2] and has a low level of clustering. As the initial condition contains many small clusters, this counterintuitively causes low-order measures of clustering [ $f_c$  and  $c_2$  in

Figs. 2(c)–2(d), and all  $c_B$  for  $B \lesssim 10$ ) to decay during OKC formation. Thus, high-order clustering information provided by the RCA is vital in identifying OKC: the rapid increase of  $|\kappa_c|^{\max}$  for  $\varepsilon(0) = 6$  in Fig. 2(e) contrasts with the cases  $\varepsilon(0) = 0, -3$ , indicating the emergence of the OKC. The demonstration of a statistically driven transfer of kinetic energy to large scales underpins the existence of an IEC in far-from-equilibrium 2DQT in scenarios with appreciable vortex clustering [19,23], and is complementary to the direct energy cascade identified in scenarios dominated by vortex-dipole recombination [13,65].

We have developed a first-principles realization of Onsager’s point-vortex model in a 2D superfluid, and observe the upscale energy transfer of 2DCT in decaying 2DQT described by the damped Gross-Pitaevskii equation. Configurational analysis of the vortex states and associated energy spectra demonstrate the emergence of an Onsager–Kraichnan condensate of quantum vortices occurring at negative temperatures in equilibrium, and as the end states of decaying 2DQT. The microcanonical sampling approach opens a new direction in the study of 2DQT, enabling systematic studies of far-from-equilibrium dynamics, energy transport, inertial ranges, and other emergent phenomena in 2DQT, and points the way to experimental realization of Onsager–Kraichnan condensation.

We thank P.B. Blakie and A.L. Fetter for valuable comments. This work was supported by The New Zealand Marsden Fund, and a Rutherford Discovery Fellowship of the Royal Society of New Zealand. B. P. A. is supported by the U.S. National Science Foundation (PHY-1205713). We are grateful for the use of NZ eScience Infrastructure HPC facilities (<http://www.nesi.org.nz>).

\*Corresponding author.

thomas.billam@otago.ac.nz

†Corresponding author.

ashton.bradley@otago.ac.nz

- [1] L. Onsager, *Nuovo Cimento Suppl.* **6**, 279 (1949).
- [2] G. L. Eyink and K. R. Sreenivasan, *Rev. Mod. Phys.* **78**, 87 (2006).
- [3] G. Boffetta and R. E. Ecke, *Annu. Rev. Fluid Mech.* **44**, 427 (2012).
- [4] P. Tabeling, *Phys. Rep.* **362**, 1 (2002).
- [5] D. Montgomery and G. Joyce, *Phys. Fluids* **17**, 1139 (1974).
- [6] D. Montgomery, W. H. Matthaeus, W. T. Stribling, D. Martinez, and S. Oughton, *Phys. Fluids A* **4**, 3 (1992).
- [7] J. Miller, *Phys. Rev. Lett.* **65**, 2137 (1990).
- [8] R. Robert and J. Sommeria, *J. Fluid Mech.* **229**, 291 (1991).
- [9] N. G. Parker and C. S. Adams, *Phys. Rev. Lett.* **95**, 145301 (2005).
- [10] S. Nazarenko and M. Onorato, *J. Low Temp. Phys.* **146**, 31 (2007).
- [11] T. L. Horng, C. H. Hsueh, S. W. Su, Y. M. Kao, and S. C. Gou, *Phys. Rev. A* **80**, 023618 (2009).
- [12] R. Numasato and M. Tsubota, *J. Low Temp. Phys.* **158**, 415 (2010).
- [13] R. Numasato, M. Tsubota, and V. S. L’vov, *Phys. Rev. A* **81**, 063630 (2010).
- [14] K. Sasaki, N. Suzuki, and H. Saito, *Phys. Rev. Lett.* **104**, 150404 (2010).
- [15] A. C. White, C. F. Barenghi, N. P. Proukakis, A. J. Youd, and D. H. Wacks, *Phys. Rev. Lett.* **104**, 075301 (2010).
- [16] B. Nowak, D. Sexty, and T. Gasenzer, *Phys. Rev. B* **84**, 020506 (2011).
- [17] B. Nowak, J. Schole, D. Sexty, and T. Gasenzer, *Phys. Rev. A* **85**, 043627 (2012).
- [18] J. Schole, B. Nowak, and T. Gasenzer, *Phys. Rev. A* **86**, 013624 (2012).
- [19] A. S. Bradley and B. P. Anderson, *Phys. Rev. X* **2**, 041001 (2012).
- [20] A. C. White, C. F. Barenghi, and N. P. Proukakis, *Phys. Rev. A* **86**, 013635 (2012).
- [21] T. Kusumura, H. Takeuchi, and M. Tsubota, *J. Low Temp. Phys.* **171**, 563 (2013).
- [22] M. Tsubota, M. Kobayashi, and H. Takeuchi, *Phys. Rep.* **522**, 191 (2013).
- [23] M. T. Reeves, T. P. Billam, B. P. Anderson, and A. S. Bradley, *Phys. Rev. Lett.* **110**, 104501 (2013).
- [24] T. W. Neely, E. C. Samson, A. S. Bradley, M. J. Davis, and B. P. Anderson, *Phys. Rev. Lett.* **104**, 160401 (2010).
- [25] T. W. Neely, A. S. Bradley, E. C. Samson, S. J. Rooney, E. M. Wright, K. J. H. Law, R. Carretero-González, P. G. Kevrekidis, M. J. Davis, and B. P. Anderson, *Phys. Rev. Lett.* **111**, 235301 (2013).
- [26] K. E. Wilson, E. C. Samson, Z. L. Newman, T. W. Neely, and B. P. Anderson, *Annu. Rev. Cold At. Mol.* **7**, 261 (2013).
- [27] R. H. Kraichnan, *J. Fluid Mech.* **67**, 155 (1975).
- [28] R. H. Kraichnan and D. Montgomery, *Rep. Prog. Phys.* **43**, 547 (1980).
- [29] M. Chertkov, C. Connaughton, I. Kolokolov, and V. Lebedev, *Phys. Rev. Lett.* **99**, 084501 (2007).
- [30] H. Xia, H. Punzmann, G. Falkovich, and M. G. Shats, *Phys. Rev. Lett.* **101**, 194504 (2008).
- [31] J. B. Weiss and J. C. McWilliams, *Phys. Fluids A* **3**, 835 (1991).
- [32] L. Campbell and K. O’Neil, *J. Stat. Phys.* **65**, 495 (1991).
- [33] M. M. Sano, Y. Yatsuyanagi, T. Yoshida, and H. Tomita, *J. Phys. Soc. Jpn.* **76**, 064001 (2007).
- [34] Y. Yatsuyanagi, Y. Kiwamoto, H. Tomita, M. M. Sano, T. Yoshida, and T. Ebisuzaki, *Phys. Rev. Lett.* **94**, 054502 (2005).
- [35] E. D. Siggia and H. Aref, *Phys. Fluids* **24**, 171 (1981).
- [36] R. H. Kraichnan, *Phys. Fluids* **10**, 1417 (1967).
- [37] C. E. Leith, *Phys. Fluids* **11**, 671 (1968).
- [38] G. K. Batchelor, *Phys. Fluids* **12**, II-233 (1969).
- [39] A. L. Gaunt, T. F. Schmidutz, I. Gotlibovych, R. P. Smith, and Z. Hadzibabic, *Phys. Rev. Lett.* **110**, 200406 (2013).
- [40] See Supplemental Material <http://link.aps.org/supplemental/10.1103/PhysRevLett.112.145301>, which provides derivations of the quantum phase  $\theta$ , the IKE spectrum and the estimated OKC transition energy used in the main text, summarizes our numerical methods, contains movies of the time evolution shown in Fig. 2, and includes Refs. [41–53].

- [41] B. C. Berndt, P. T. Joshi, and B. M. Wilson, *Glasg. Math. J.* **22**, 199 (1981).
- [42] A. L. Fetter, *J. Low Temp. Phys.* **16**, 533 (1974).
- [43] A. S. Bradley, C. W. Gardiner, and M. J. Davis, *Phys. Rev. A* **77**, 033616 (2008).
- [44] C. W. Gardiner and M. J. Davis, *J. Phys. B* **36**, 4731 (2003).
- [45] M. T. Reeves, B. P. Anderson, and A. S. Bradley, *Phys. Rev. A* **86**, 053621 (2012).
- [46] S. J. Rooney, T. W. Neely, B. P. Anderson, and A. S. Bradley, *Phys. Rev. A* **88**, 063620 (2013).
- [47] O. Törnkvist and E. Schröder, *Phys. Rev. Lett.* **78**, 1908 (1997).
- [48] M. Kobayashi and M. Tsubota, *Phys. Rev. Lett.* **97**, 145301 (2006).
- [49] J. C. McWilliams, *J. Fluid Mech.* **219**, 361 (1990).
- [50] Z. Xiao, M. Wan, S. Chen, and G. Eyink, *J. Fluid Mech.* **619**, 1 (2009).
- [51] J. P. Boyd, *Chebyshev and Fourier Spectral Methods* (Dover, New York, 2000), 2nd ed.
- [52] P. B. Blakie, *Phys. Rev. E* **78**, 026704 (2008).
- [53] V. Shukla, M. Brachet, and R. Pandit, *New J. Phys.* **15**, 113025 (2013).
- [54] We use the term “2D BEC” to denote a BEC externally confined in one dimension such that the vortex dynamics are effectively 2D [55], while phase coherence is preserved, avoiding the Berezinskii-Kosterlitz-Thouless regime [56,57].
- [55] S. J. Rooney, P. B. Blakie, B. P. Anderson, and A. S. Bradley, *Phys. Rev. A* **84**, 023637 (2011).
- [56] Z. Hadzibabic, P. Kruger, M. Cheneau, B. Battelier, and J. Dalibard, *Nature (London)* **441**, 1118 (2006).
- [57] P. Clade, C. Ryu, A. Ramanathan, K. Helmerson, and W. D. Phillips, *Phys. Rev. Lett.* **102**, 170401 (2009).
- [58] We use energy tolerance  $\pm \max(0.05\epsilon, 5 \times 10^{-3})$ . Ensemble sizes in Fig. 1 are  $10^2$  [magenta circles in (c)],  $10^4$  [other curves in (c),(d)],  $10^7$  [structure function in (a)], and  $10^3$  [other curves in (a),(b)].
- [59] C.-k. Chan, D. Mitra, and A. Brandenburg, *Phys. Rev. E* **85**, 036315 (2012).
- [60] M. Tsubota, K. Kasamatsu, and M. Ueda, *Phys. Rev. A* **65**, 023603 (2002).
- [61] A. A. Penckwitt, R. J. Ballagh, and C. W. Gardiner, *Phys. Rev. Lett.* **89**, 260402 (2002).
- [62] P. B. Blakie, A. S. Bradley, M. J. Davis, R. J. Ballagh, and C. W. Gardiner, *Adv. Phys.* **57**, 363 (2008).
- [63] We have confirmed that quantitatively similar vortex dynamics occur in simulations of the projected Gross-Pitaevskii equation [62,66–68] for  $\gamma = 0$ , demonstrating that Hamiltonian dynamics also lead to OKC formation for  $\epsilon(0) = 6$  [40].
- [64] Note that the OKC is not composed of the same vortices at all times; the condensate gradually exchanges vortices with the uncorrelated background.
- [65] P. M. Chesler, H. Liu, and A. Adams, *Science* **341**, 368 (2013).
- [66] M. J. Davis, S. A. Morgan, and K. Burnett, *Phys. Rev. Lett.* **87**, 160402 (2001).
- [67] M. J. Davis and P. B. Blakie, *Phys. Rev. Lett.* **96**, 060404 (2006).
- [68] T. P. Simula and P. B. Blakie, *Phys. Rev. Lett.* **96**, 020404 (2006).